Multi-body elastic simulation of a go-kart: Correlation between frame stiffness and dynamic performance

Article *in* International Journal of Automotive Technology · August 2010

DOI: 10.1007/s12239-010-0057-6

CITATIONS
10

READS
9,801

1 author:

G. Mirone
University of Catania
66 PUBLICATIONS **1,130** CITATIONS

SEE PROFILE

International Journal of Automotive Technology, Vol. 11, No. 4, pp. 461–469 (2010)
DOI 10.1007/s12239–010–0057–6

1229–9138/2010/053–03

MULTI-BODY ELASTIC SIMULATION OF A GO-KART: CORRELATION BETWEEN FRAME STIFFNESS AND DYNAMIC PERFORMANCE

G. MIRONE*

Dipartimento di Ingegneria Industriale e Meccanica, Università di Catania, Viale A. Doria 6, 95125, Catania, Italy

(Received 30 March 2009; Revised 2 October 2009)

ABSTRACT–The elastic response of a vehicle to an applied force determines the dynamic performance, comfort, and support of the vehicle, where the elastic response depends primarily on the stiffness of the frame/chassis. Significant variations in the dynamic response of a vehicle are typically achieved with suitable shock absorbing systems, which contribute significantly to whole body flexibility. The defining feature of a go-kart is the lack of devices capable of absorbing shock and dampening vibration. The tires and body of a go-kart, which consist of a frame of welded beams, must also function as a shock absorption system. The objective of this study was to reproduce the elastic behavior of a commercially available Italian go-kart by modeling the frame in a multibody ADAMS environment and to determine the effect of elastic features on the dynamic performance of the vehicle. Frame stiffness was assessed by applying a static torsion moment, while the circular trajectory of the go-kart was evaluated at different speeds and steering wheel angles. The proposed multibody, flexible model was validated by comparing the static and dynamic response of the go-kart in simulated and experimental analyses. The results of numerical simulations demonstrated that this method may be extended to the design of customized go-kart frames and to the tuning of go-karts for specific racing conditions.

KEY WORDS : Go-kart, Slip angle, Frame stiffness, Handling

1. INTRODUCTION

The go-kart was developed to provide a low-cost vehicle for young racers. Go-karts are simple vehicles with limited components and subsystems, and are used for both training and competition.

Although research on go-karts provides interesting information and could potentially yield new technologies, from an engineering standpoint, go-kart related literature is relatively scant. Nevertheless, the effect of frame characteristics on specific dynamic responses has been studied over the last few years (Guglielmino *et al*., 2000; Mirone, 2003; Ponzo and Renzi, 2004; Muzzupappa *et al.*, 2005; Biancolini *et al*., 2007).

The main simplifications introduced into the design of a go-kart include the removal of shock absorbing systems and rigid rear axles that connect the driving wheels.

The removal of these features may dramatically reduce the dynamic performance because a rigid connection between the body and wheels results in a large load transfer and poor maneuverability (Cianetti *et al.*, 1994; Kim and Kim, 2007; Lee and Yoo, 2009). Moreover, the lack of any mechanic differential between the two driving wheels leads to uniform peripheral tire speeds, which results in poor performance with respect to curvilinear trajectories. Nevertheless, if the flexibility of the frame and rear axle is calibrated with tire behavior, go-karts are very agile and capable of undergoing large lateral accelerations.

The ideal tuning of a frame depends on the current conditions; thus, to maintain optimal frame stiffness during an entire race, an active frame or pilot-operated tuning device can be utilized, where the configuration of the suspension is modified in real time.

Complex regulation systems are not available for go-karts, and limited tuning may be performed by employing rear axles with different diameters and lengths. Thus, the configuration of a go-kart is a compromise between the requirements of many conditions for a single race.

It is clear that the simplifications in go-kart design introduce substantial difficulties.

In this work, a commercially available go-kart was experimentally tested and modeled with ADAMS software. To validate the model, the static-dynamic behavior of a go-kart was simulated numerically. Theoretical and experimental results were in good agreement; thus, the proposed analysis was suitable for predicting the performance of go-karts and for the design of frames under dynamic racing conditions.

2. STATIC MODELING OF THE GO-KART FRAME

As shown in Figure 1, the frame of the go-kart used in this study was made of welded steel tubes with different dia-

**Corresponding author.* e-mail: gmirone@diim.unict.it

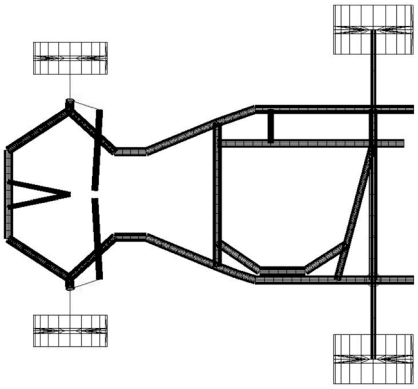

Figure 1. Go-kart frame.

Table 1. Principal dimensions of the go-kart frame.

Pitch (mm)	Front track (mm)	Rear track (mm)	Caster angle (deg)	Kingpin angle (deg)	Front tire radius (mm)	Rear tire radius (mm)
1068	960	1160	12.8	6.5	130	140

meters and thicknesses. The dimensions of the go-kart are provided in Table 1:

The steel used in the frame was 25CrMo4 and ASTM A284, and the diameters and thickness of the tubes ranged from 14 to 30 mm and 1.5 to 2 mm, respectively.

The total weight of the vehicle and the pilot was 140 kg, where 57% of the total weight was distributed on the rear tires and 43% was distributed on the front tires under static conditions.

The frame was modeled with flexible links capable of simulating the static and dynamic behavior of beam-like elastic bodies. After various preliminary analyses, each straight beam was divided into sections with a length equal to the diameter of the outer tube to determine the appropriate amount of segregation. The division of the beams provided acceptable accuracy in the evaluation of frame elastic displacements, but significant time was required for each analysis.

The multibody model of the naked frame was statically validated by simulating a series of experimental tests, where torsional loads were applied to the front tube of the frame and the rear end was fully constrained to a rigid wall.

As shown in Figure 2, the center of the front bar of the frame was hinged at a fixed distance from the ground to avoid flexural displacements.

Micrometers were placed at eight specific locations along the frame to measure the vertical displacement due to the applied loads, as shown in Figure 2. Points 1, 2, 7 and 8 corresponded to the front steering hubs and the rear axle, respectively. Two different magnitudes of torsion were applied to assess the behavior of load-displacement in the frame.

Figure 3 confirmed that the behavior of the frame was linear under all applied loads. Linearity was indicated by the complete coincidence of displacement data (normalized with respect to the applied torque) at 35 and 70 Nm of torque. Furthermore, the results indicated that stiffness was significantly lower in the front end tube. In this zone, the frame was reduced to two parallel tubes, which were closer to the longitudinal axis of the frame than other areas.

In other words, the region of the frame near points 3 and 4 is primarily responsible for the torsional compliance of the entire frame.

The application of 70 Nm of torque was simulated with the ADAMS numerical model by applying two fixed constraints at the rear of the kart, a rotational constraint (a hinge with a rotational axis parallel to the frame's longitudinal axis) in the midsection of the front transverse tube, and a torque of 70 Nm to the midsection of the tube.

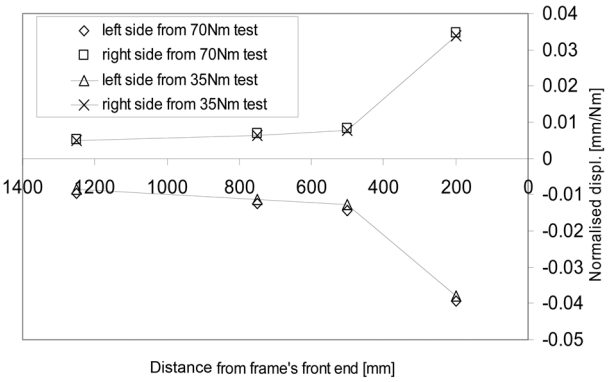

Figure 3. Vertical displacement at frame control points under torsional stress.

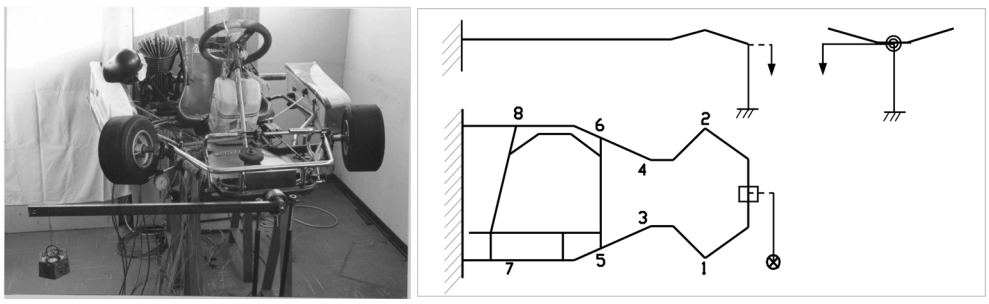

Figure 2. Experimental static tests to determine the torsional stiffness of the frame.

Table 2. Experimental and theoretical elastic displacement (70 Nm torque).

Vertical displ. [mm]	Point 1	Point 2	Point 3	Point 4	Point 5	Point 6
Experimental	−2.75	2.42	−1	0.58	−0.87	0.48
Theoretical	−2.5	2.4	−0.9	0.65	−0.8	0.5

The theoretical displacement at the control points was compared to the experimental results in Table 2.

An acceptable agreement was obtained, confirming that the static model of the frame was appropriate.

By inducing relative rotation between the rear axle and the imaginary line between the axes of the front tires at a null steering angle, a meaningful quantification of frame stiffness was obtained from the applied torsion. The experimental and theoretical stiffness of the frame, obtained from the aforementioned analysis, was 166 and 161 Nm/deg, respectively.

The multibody model of the go-kart frame was validated with respect to static elastic response and was completed by modeling the steering system, rear axle, tires, driving torque on the rear axle, and motion law for the steering wheel, as well as the mass of the pilot, fuel tank and engine.

3. DYNAMIC MODELING OF THE COMPLETE VEHICLE

In the model of the steering system, the front tires were considered hinges, the spherical joints were considered rigid bodies, and the steering rods and steering wheel shaft were considered elastic beams. Verification of the cinematic response of the model was performed by comparing tire movement at five steering angles and the movement of the experimental go-kart. A maximum discrepancy of 7% was observed at high angles (40~50 degs).

The rear axle was connected to the frame by two hinges placed at the ball-bearings, while the pilot, fuel tank and engine were simulated as rigid bodies with a given weight, gravity center and inertia. The pilot's weight was subdivided into two parts including the legs, which were placed in a nearly horizontal position (15 Kg, where the center of gravity was halfway between the base of the pelvis and knees), and the torso and head (50 kg, where the center of gravity was placed under the sternum bone). Each of these rigid parts was linked to locations in the frame, including the point of attachment for the seat, steering wheel and seat-belt.

To validate the dynamic behavior of the go-kart, fully circular turns at constant speeds and steering angles were simulated in the multibody model. The same maneuvers were conducted experimentally and were compared to the simulated turns.

To ensure that the desired speed was maintained, a specific amount of torque was required to compensate for the friction between the joints and tire-rod. In the actual maneuver, torque is provided by the pilot, who acts on the throttle and brakes. In the simulation, torque acted on the rear axle, where the magnitude of torque was proportional to the difference between the effective current axle speed and the target axle speed (V_{eff}-V_{targ}).

A proportionality constant between the applied torque and delta-speed was implemented. As a result, the maximum torque, which corresponded to a delta-speed of 15 m/s, did not exceed that of an average two-stroke engine at 35 BHP and 12000 RPM.

In each simulation, the go-kart traveled along a straight path for the first 0.2 or 0.4 seconds. Next, a progressive rotation at a rate of 25 degrees per second was imposed on the steering wheel until the desired angle was achieved. The selected angle was maintained for two or three circular trajectories, and the results were evaluated. In the experimental study, an actual go-kart was subjected to the same sequence of events.

The tire model utilized in the theoretical study was the *UATire* model, which can be used for handling/comprehensive slip analyses. The main assumptions of this model

Table 3. Parameters required for tire definition.

Parameter	Meaning
–	Tire width
R1	Outer radius of the unloaded (undeformed) tire
R2	Inner radius of the tire (outer radius of the tire hub)
CN	Tire radial stiffness
Cs	Tangent of the curve "longitudinal load-vs.-slip ratio", evaluated at null slip ratio
Cα	Tangent of the curve "lateral load-vs.-slip angle", evaluated at null slip angle
Cγ	Tangent of the curve "lateral load-vs.-incl. angle", evaluated at null incl. angle
CRR	Eccentricity of the vertical force on the contact patch (rolling resist. moment arm)
RDR	Relative damping ratio
U0	Friction coefficient at null comprehensive slip
U1	Friction coefficient at full comprehensive slip

include a rectangular contact patch and a parabolic distribution of pressure across the contact patch, where tire response is modeled as a beam on an elastic foundation. The input parameters required to characterize each tire according to the *UATire* model are described schematically in Table 3.

The majority of these constants can be obtained from experimental tests with specific equipment. However, the machinery necessary to conduct these tests was not available, and the appropriate data was not found in the literature. Thus, characterization of go-kart tires was accomplished indirectly.

In circular trajectories at a constant speed and steering angle, the effect of *Cs* is negligible because the longitudinal slip and corresponding contact forces are low.

Under the aforementioned conditions, $C\gamma$ does not have a significant effect because the lateral force due to the inclination angle is many times lower than the lateral force due to the lateral slip angle. Thus, *Cs* and $C\gamma$ were based on the $C\alpha$ of sport automotive tires

CRR was estimated by measuring the distance covered by the vehicle before coming to a complete stop without the assistance of traction or braking at different initial speeds. The estimation of *CRR* was approximate because the effects of friction in the transmission chain were included.

RDR was determined on the basis of a qualitative estimation at different vertical loads. RDR varies substantially with tire pressure and does not have a significant effect on the dynamic equilibrium of a vehicle traveling at a constant speed in circular trajectories.

The friction coefficients U0 and U1 were estimated according to the hypothesis of negligible load transfers. Specifically, U0 and U1 were obtained by measuring the distance covered during braking at the sliding limit or under full slip conditions at various speeds.

$C\alpha$ was the most influential coefficient in the simulated conditions and was evaluated for rear and front tires.

By approximating a linear function, the relationship between moderate slip angle and lateral forces (1) was obtained. As shown in Figure 4, the rotational equilibrium equation (2) provided a relationship between the $C\alpha$ of the front and rear tires, which reduced the number of unknowns to one.

$$Y_1 = C_{\alpha\_rear} \cdot \alpha_{rear}; \quad Y3 \cong Y4 = C_{\alpha\_front} \cdot \alpha_{front}; \tag{1}$$

$$Y1 \cdot a - (Y3 + Y4) \cdot b = 0; \tag{2}$$

By substituting Equation (1) into Equation (2), the ratio between $C\alpha$ of the rear and front tires was obtained.

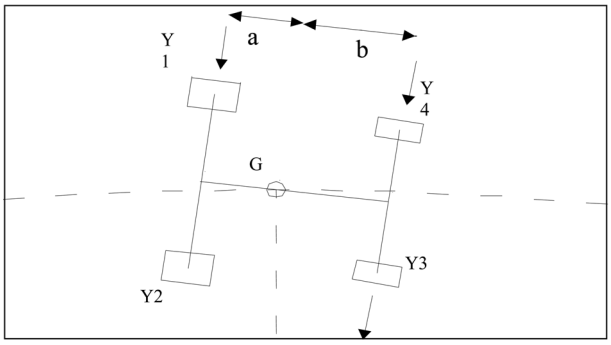

Figure 4. Lateral forces in circular paths at a constant speed.

$$C_{\alpha\_rear} \cdot \alpha_{rear} \cdot a - 2 \cdot C_{\alpha\_front} \cdot \alpha_{front} \cdot b = 0;$$

$$\Rightarrow \frac{C_{\alpha\_rear}}{C_{\alpha\_front}} = \frac{2b}{a} \cdot \frac{\alpha_{front}}{\alpha_{rear}} \cong \frac{2b}{a} = 2.6; \tag{3}$$

In Equation (2), the load Y2 was assumed to be null because the rear tire on the internal side of the curve was not in contact with the surface of the ground. To compensate for the lack of differential, go-karts are designed to minimize contact between the rear tire and the ground.

The above assumptions reduced the number of unknown tire parameters to one, and the remaining parameter was obtained by trial and error. Specifically, each cycle consisted of simulations at a given speed and steering angle, where the experimental results of the analysis were known (radius of the circular trajectory). Iterations were repeated by varying the initially random value of $C\alpha$ until the analysis agreed with the experimental data. After an appropriate value of $C\alpha$ and an accurate simulation was obtained, other experimental tests (different combinations of speed-steering angle) were conducted. Overall, the results suggested that the properties of tires were successfully characterized.

The set of coefficients determined by this procedure are shown in Table 4, while the corresponding tire behavior expressed as the UATire subroutine in terms of lateral force vs. slip angle is shown in Figures 5 and 6, as a function of vertical load (*Fz*).

Tire characterization was the final step in the dynamic modeling of the go-kart. The complete model of the go-kart was used to perform seven analyses simulating several experimental tests.

Table 4. Estimated tire parameters.

Parameter	width *mm*	R1 mm	R2 mm	CN N/mm	Cs N	Cα N/rad	Cγ N/rad	CRR mm	RDR –	U0 –	U1 –
Rear tires	200	140	73	200	2500	10000	2000	30	0.2	1.8	0.4
Front tires	130	130	63	150	1000	4000	800	20	0.1	1.8	0.4

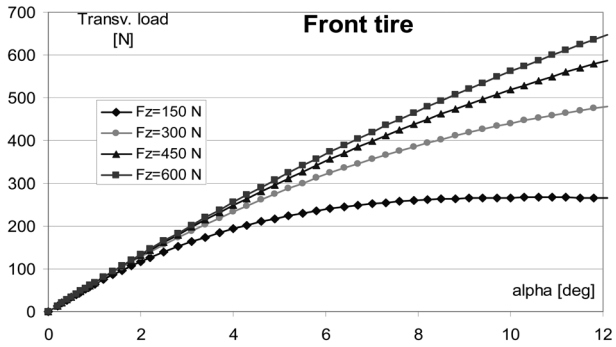

Figure 5. Transverse forces vs. slip angle at four vertical loads for front tires.

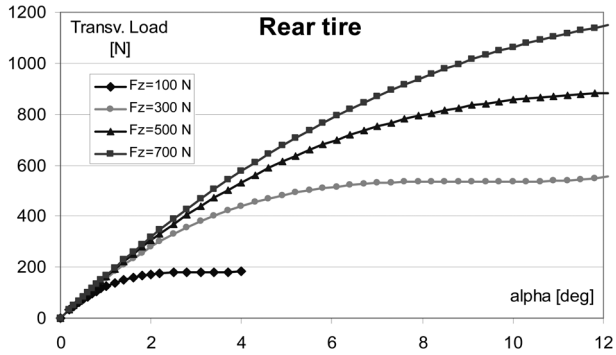

Figure 6. Transverse forces vs. slip angle at four vertical loads for the rear tires.

4. EXPERIMENTAL–NUMERICAL COMPARISON FOR CIRCULAR TRAJECTORIES AT CONSTANT SPEED

As shown in Figure 7, the go-kart was equipped with a digital odometer on the right front wheel and a protractor on the steering wheel to assist the pilot in controlling the speed and steering wheel angle. A bottle containing white liquid was placed behind the pilot's seat, and the liquid was allowed to drip from the bottle as the go-kart progressed.

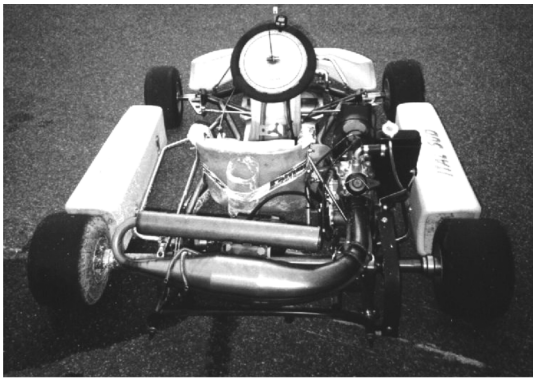

Figure 7. Instrumented go-kart.

As a result, the liquid marked the trajectory of the go-kart on the surface of the road.

The test consisted of a short acceleration ramp and seven circular trajectories at a constant speed and steering angle. The speed and steering wheel angles investigated in this study were 16 km/h at 15 deg, 21.5 km/h at 20 deg, 33.5 km/h at 20 deg, 15 km/h at 30 deg, 22 km/h at 30 deg, 19 km/h at 40 deg, and 15 km/h at 50 deg.

Simulations were conducted at initial speeds and steering angles identical to those used in actual experiments. To compensate for rolling resistance and to maintain a constant speed, the theoretical analysis included torque on the rear axle. Moreover, after an initial steering transition period, sufficient time was allotted to complete at least one circular trajectory.

The time interval of the theoretical analysis was approximately 10^{-3} seconds, resulting in 7000 to 21000 intervals within the seven simulated conditions.

Figure 8 shows a typical output of a simulated circular trajectory (at 22 km/h and 30 deg). The trajectory displays successive positions assumed by the center of gravity of the pilot's torso.

The most intuitive comparison of experimental and theoretical results was made by examining the radii of go-kart trajectories, as reported in Table 5 and Figure 9.

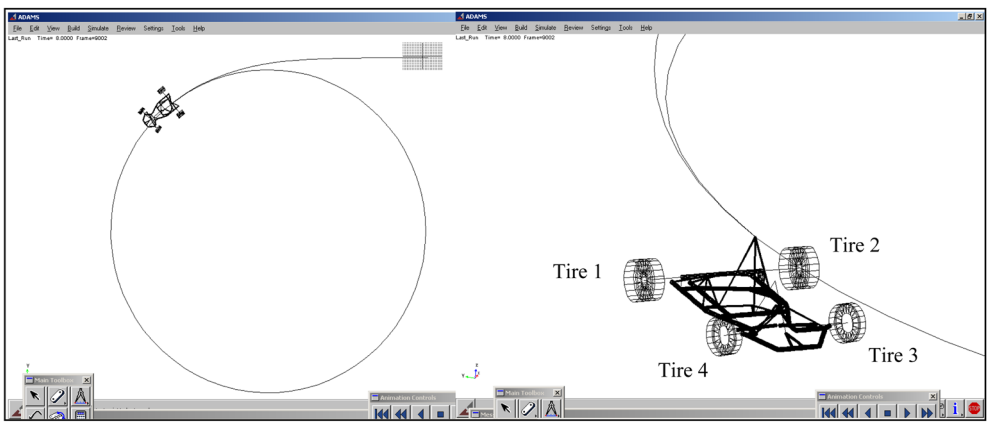

Figure 8. ADAMS Simulation of the circular trajectories.

Table 5. Comparison of theoretical and experimental results (circular trajectories at various speeds and steering angles).

Speed [km/h]	Steering angle [°]	Centripetal acceleration (exp.) [g]	Radius of the experimental traject. [m]	Radius of the numerical traject. [m]	Error
16	15	0.16	12.4	11.7	−5.6%
15	30	0.30	6.0	5.8	−3.3%
21.5	20	0.39	9.4	9.1	−3.2%
22	30	0.56	6.7	6.1	−8.9%
15	50	0.59	3.0	2.9	−3.3%
19	40	0.65	4.4	4.1	−6.8%
33.5	20	0.94	9.4	10.1	−7.4%

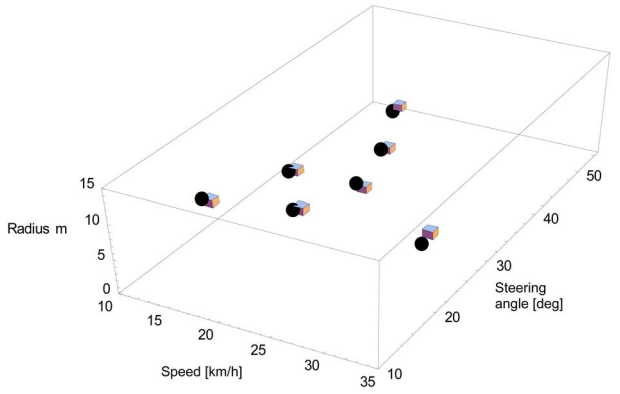

Figure 9. Graphical representation of theoretical and experimental results (radii of circular trajectories at various speeds and steering angles).

The torque applied to the rear axle adequately balanced the rolling resistance of the tires, producing very small differences (<0.5 km/h) between the effective and target speed.

The radii of predicted trajectories were in agreement with those determined experimentally (maximum error less than 9%). A significant portion of error could be due to slight differences between the steering cinematic chain in the model and the actual chain. For instance, further analyses performed with steering angles modified by 2~3 degrees led to the accurate prediction of trajectory radii.

As shown in Figure 9, the proposed theoretical model reproduced the *speed-steering angle* and *radius* of *curvature* in triplicate. Even with different combinations of variables, the results were in agreement with the experimental data.

5. ANALYSIS OF RESULTS

The response of the multibody model under different simulated conditions provided useful information on the dynamic behavior of go-karts, including the load transfer and frame torsion in circular trajectories.

As shown in Figures 10~12, in six of the seven simulations, the vertical load acting on the tires was transferred from the internal side of the curve to the outer side due to centripetal acceleration (expressed for each plot as a fraction of the acceleration of gravity) and the steering angle. In the figure, tires 1, 2, 3 and 4 indicate the rear external, rear internal, front internal and front external tires, respectively.

Longitudinal acceleration of the go-kart was negligible because the torque required to maintain a constant speed was low. Thus, the static distribution of vertical forces varied horizontally, without any front-rear load transfer.

Alternatively, the lateral load transfer on tires was affected by the steering angle and centripetal acceleration.

The contribution of the steering motion to the vertical load transfer was due to the caster angle, which is typical in go-karts. The effect of the caster angle was clearly visible when the steering wheel was rotated under static conditions (null speed, no pilot on board, frame not deformed elastically). Under these conditions, one of the four tires tended to rise off the surface of the road. This behavior is intentional and is included in the kart design because it facilitates the unloading of the rear tire on the internal side of the curve, creating an effect similar to that of a differential.

Lateral acceleration transfers vertical loads toward the external side of the trajectory in the front and rear tires almost equally. In theory, if the center of gravity was placed halfway between the front and rear axles, a difference in the load transfer of the front and rear tires would not be observed.

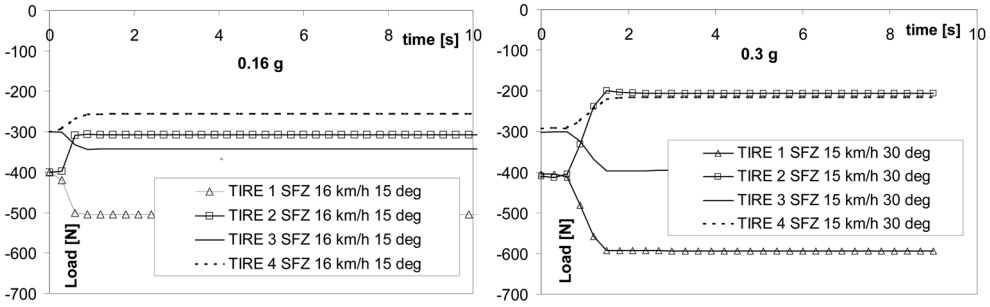

Figure 10. Vertical load transfer at acceleration values of 0.16 and 0.3 g.

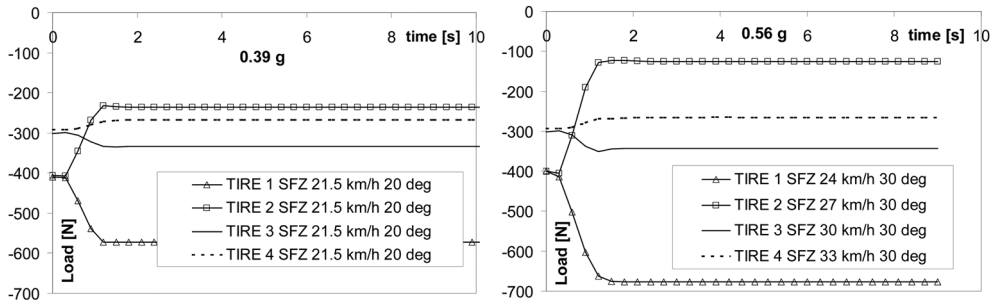

Figure 11. Vertical load transfer at acceleration values of 0.39 and 0.56 g.

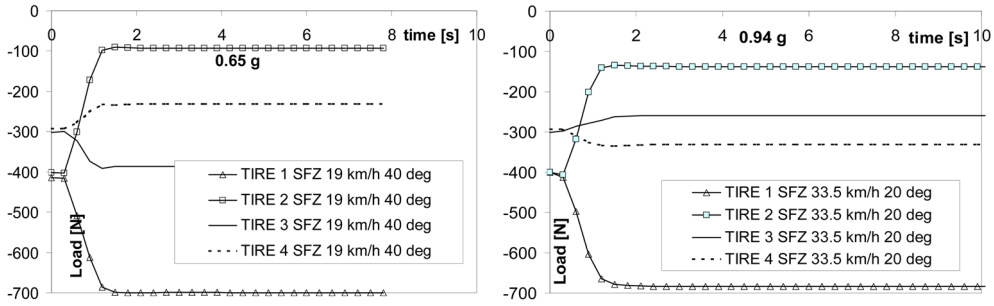

Figure 12. Vertical load transfer at acceleration values of 0.65 and 0.94 g.

On the contrary, the motion of the steering system causes different load transfers in the front and rear tires. In the front tires, the vertical load was shifted towards the internal side of the trajectory, opposing the effect of lateral acceleration. Alternatively, in the rear tires, the load was shifted towards the external side, increasing the effect of lateral acceleration.

As shown in Figures 10~12, the effect of steering angle exceeded that of centrifugal force in the front tires at low and medium lateral accelerations (from 0.16 g up to 0.65 g), which caused the internal front tire (n. 3) to carry a higher load than the external tire (n. 4). A comparison of the simulated front tire load at a steering angle of 30 degrees and an acceleration of 0.3 g and 0.56 g revealed that centrifugal force tended to increase the load on the external side of the trajectory, reducing the unbalance in the front tires caused by the steering angle. In the last simulation, the external front tire (n. 4) carried a larger load than the internal tire (n. 3) because the effect of centrifugal force at a lateral acceleration of 0.94 g exceeded the effect of steering wheel rotation at 20 degrees.

In simulations conducted at 0.3 and 0.39 g, the centrifugal force and the steering wheel angle increased the load on the external side of the trajectory. Moreover, the rear tires carried a nearly identical load, indicating that an additional rotation of 10 degrees (first case) had almost the same effect as 0.09 g of centripetal acceleration (second case) on the vertical load of the rear tires.

Saturation behavior with respect to load transfer on the rear tires did not allow the maximum load to exceed 700 N on the external rear tire.

Finally, Figure 13 displays the torsion angle of the frame, evaluated by the vertical displacement of the tire attachment points.

The data in Figure 13 revealed that the elastic deformation of the frame depended exclusively on the steering angle. For instance, the torsion angle of the frame increased with an increase in steering angle, and the centrifugal force did not affect frame torsion. In fact, the fourth and the fifth simulations confirmed that equal lateral accelerations (56% and 59% of g) and different steering angles (30 and 50 degs) induced very different torsion angles (0.57 deg and 0.87 deg). On the contrary, the second and fourth curves of Figure 13 confirmed that different accelerations (30% and 56% of g) at an identical steering angle (30 degrees) induced the same amount of frame torsion (0.57 degrees). Identical trends were observed in simulations conducted at a steering angle of 20 degrees. For instance, despite vari-

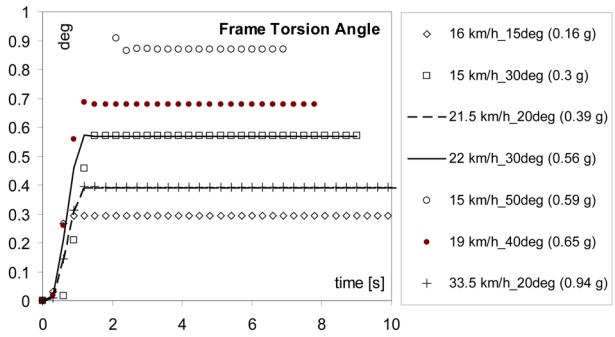

Figure 13. Torsion angle of the frame in all seven simulations.

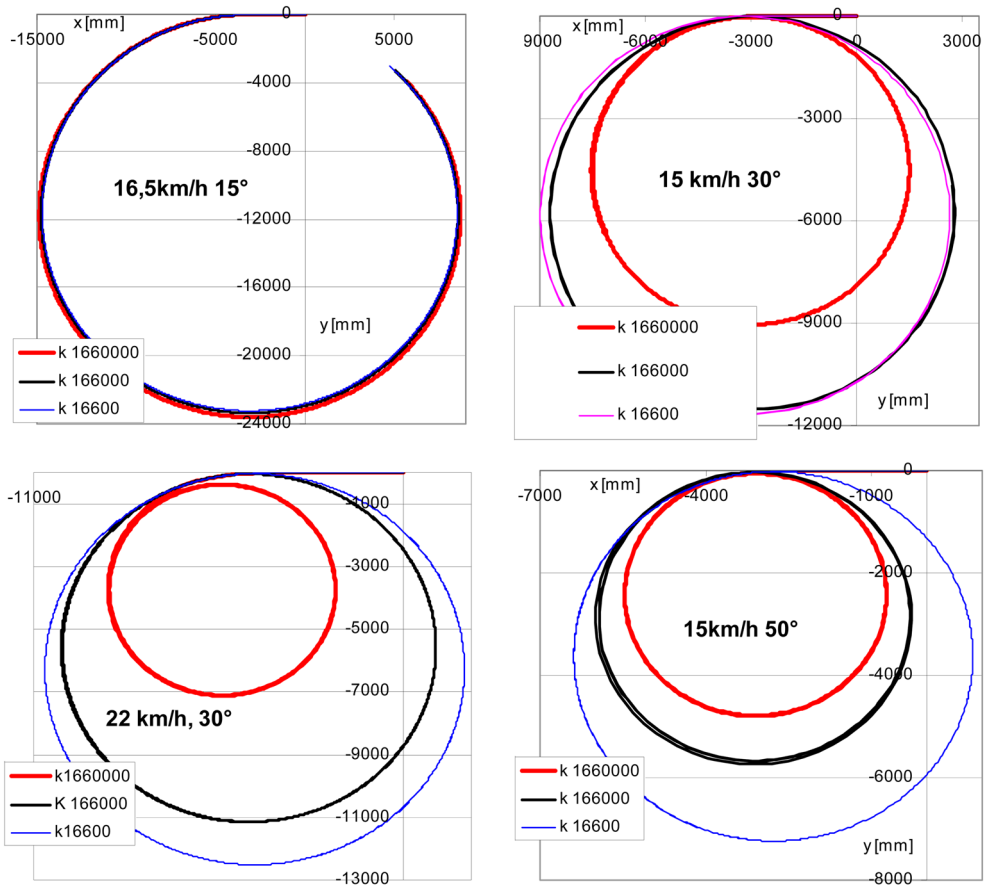

Figure 14. Effect of frame stiffness on the trajectory.

ations in lateral acceleration (from 0.39 to 0.94 g), frame torsion remained constant at approximately 0.4 degrees.

To further simply the tuning procedure, a new basic model of the kart was assembled by substituting the elastic frame with two rigid parts connected by a torsion spring, which concentrates the compliance of the entire frame on its longitudinal axis (points 3 and 4 of Figure 2).

To determine the effect of frame stiffness on the performance of the go-kart, the spring stiffness was set to 165000 Nmm/deg, which corresponded to a frame stiffness of 16500.

Speeds and steering wheel angles used in the original experiments were also used to simulate the response of simplified frames.

The resulting trajectories are displayed in Figure 14.

The theoretical response of the simplified frame and the stiffness of the actual frame were similar to the experimental response, indicating that the total stiffness between the rear and front tires was more important than the distribution of stiffness along the longitudinal axis of the frame.

Variations in the trajectory due to increased or decreased frame stiffness were clearly visible, confirming that multibody analyses are able to estimate the interaction between the elasticity of the frame and the dynamic behavior of the go-kart.

The validation of the model indicated that numerical analyses can quantify the effect of frame stiffness on load transfer and the dynamic performance of the vehicle.

Many different motion sequences can be modeled, allowing the prediction of corresponding go-kart responses and frame optimization for specific conditions.

6. CONCLUSIONS

Experimental tests were conducted on a go-kart to determine frame stiffness and the radius of circular trajectories at selected speeds and steering angles.

Multibody modeling of the go-kart was achieved by taking into account the elastic properties of the frame. The results indicated that elastic components were primarily responsible for the dynamic performance of go-karts.

The tires were characterized by adopting a set of hypotheses based on the dynamic conditions in experimental tests. Theoretical and experimental data were compared to validate the model's response and the proposed tire parameters. The results indicated that a maximum error of 9% was observed in the radii of circular trajectories.

An analysis of the theoretical results provided interesting

aspects of go-kart behavior with respect to tire load transfer and frame torsion, suggesting that a simplified frame representation may be useful for a first evaluation of frame response under a set of dynamic conditions. The effect of frame stiffness on the trajectories at a fixed speed and steering angle was evaluated, confirming that simplified models are able to predict the effect of frame configuration on the dynamic performance of the vehicle.

Further developments of the model should include a rigorous characterization of the tires; however, the results indicated that the model can be used successfully in the design and tuning of go-kart frames and tires. Thus, the model can be applied to optimize the go-kart for specific conditions.

REFERENCES

Biancolini, M. E., Cerullo, A. and Reccia, L. (2007). Design of a tuned sandwich chassis for competition go-kart. *Int. J. Vehicle Design*, **44**, 360–378.

Cianetti, F., Di Pietro, G., Guglielmino, E. and La Rosa, G. (1994). Structural optimization of a composite material racing-car body. *4th Int. Conf. New Design Frontiers for More Efficent, Reliable and Ecological Vehicles*, Firenze.

Guglielmino, E., Guglielmino, I. D. and Mirone, G. (2000). Caratterizzazione numerico-sperimentale di un go-kart da competizione. Atti del XXIX° Convegno AIAS, Lucca, 57–68.

Kim, K. C. and Kim, C. M. (2007). Analysis process applied to a high stiffness body for improved vehicle handling properties. *Int. J. Automotive Technology* **8**, **5**, 629–636.

Lee, J. H. and Yoo, W. S. (2009). Predictive control of a vehicle trajectory using a coupled vector with vehicle velocity and sideslip angle. *Int. J. Automotive Technology* **10**, **2**, 211–217.

Mirone, G. (2003). Mulibody modelisation of a go-Kart with flexible frame: simulation of the dynamic behaviour and experimental validation. *Proc. JSAE Int. Body Engineering Conf. 2003*.

Muzzupappa, M., Matrangolo, G. and Vena, G. (2005). Experimental and numerical analysis of the Go-Kart frame torsional behaviour. *XVII Ingegraf – XV ADM. Seville.*

Ponzo, C. and Renzi, F. (2004). Parametric multi-body analysis of kart dynamics. *The 30th FISITA World Cong. 2004*, Barcelona, Spain.